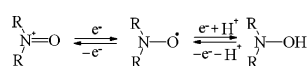


Nitroxyl Radicals for Studying Electron Transfer**

Tamar Eliash, Antonio Barbon,* Marina Brustolon, Mordechai Sheves, Itzhak Bilkis, and Lev Weiner*

Electron transfer (ET) is a fundamental process underlying many chemical and biochemical reactions.^[1,2] Over the years, a powerful arsenal of physicochemical methods has been employed to study ET. Although the principal methods employed have been optical,^[2] other methods have been used, and in particular scanning electrochemical microscopy.^[3] Nevertheless, there is still a need for novel and/or more flexible experimental approaches to the quantitative study of ET in both biological and chemical systems.

Herein we make use of electron paramagnetic resonance (EPR) spectroscopy for studying ET in chemical and biological systems. It was established earlier that stable nitroxyl radicals (SNRs) can undergo redox reactions (Scheme 1) with concomitant conversion into diamagnetic species, that is, the



Scheme 1. Oxidation and reduction processes of stable nitroxyl radicals.

corresponding hydroxylamine and oxoammonium cation.^[4] This permits use of SNRs to monitor the ET process by following disappearance of their EPR signals. However, this approach has never been used to study the kinetics of ET reactions.

A major problem in ET studies on biological systems is associated with the selective switching on and off of the electron donor/acceptor pair. This problem was successfully

solved in studies on ET in complexes of ruthenium with cytochromes and blue copper proteins. Time-resolved optical spectroscopy utilized the laser flash-quench triggering method to excite the bound ruthenium complex that served as one donor/acceptor. The endogenous Fe³⁺/Fe²⁺ or Cu²⁺/Cu⁺ metal centers were the complementary acceptor/donors that served as endogenous antennae.^[2,5] However this approach is limited to metal containing proteins. We have adopted a similar photo-switching approach, together with time-resolved EPR, for the donor/acceptor pair SNR/Ru³⁺. SNRs can indeed be oxidized by Ru³⁺, as earlier shown for TEMPO using laser flash photolysis.^[4] The oxidation potential of 1.06 V versus Ag/AgCl,^[6] for a [Ru(bpy)₃]²⁺/[Ru(bpy)₃]³⁺ couple, is well above that of a typical nitroxide moiety, namely $E_{1/2} \approx 0.6$ V.^[4,7] The advantage of using a SNR is that the spin probe can be introduced at a desired location on the protein studied by use of site-directed spin labeling.^[8] In the present study, which employs bacteriorhodopsin (bR), we further took advantage of the observation that bound Ca²⁺ ions can successfully be replaced by various bulky metal complexes, including [Ru(bpy)₃]²⁺.^[9] An additional reason for using bR as a model protein for testing the proposed approach is the recent finding that bR in the solid state shows a high propensity to conduct electric currents.^[10]

The experimental procedure (see the Supporting Information for details) involved use of a laser pulse to raise [Ru(bpy)₃]²⁺ to an excited state, [Ru*(bpy)₃]²⁺, which was quickly oxidized to [Ru(bpy)₃]³⁺ by ammonium persulfate. In turn, [Ru(bpy)₃]³⁺ oxidizes the SNR to the corresponding oxoammonium cation (Scheme 1). The subsequent decrease of the SNR was then followed in time by monitoring the continuous-wave (cw) EPR intensity of the SNR.

Initially, we studied ET from a free SNR, 3-carboxy-2,2,5,5-tetramethylpyrrolidine-*N*-oxyl (3-carboxyproxyl), to a free [Ru(bpy)₃]³⁺. We report data obtained in two solutions characterized by different viscosities: water/ethanol 1:1, as a low-viscosity solvent, and water/glycerol 3:7 as a high-viscosity solvent. Figure 1 shows that the rate of disappearance of the SNR cw-EPR signal for the aqueous ethanol solution depends on the concentrations of both the reagents. The time profile is characterized by an initial lag time, followed by a decay which brings the intensity to a plateau. The observed uncorrelated oscillation of the baseline does not affect these features, and the analyses of different samples are consistent within errors. Analogous trends were seen in the aqueous glycerol, but the reaction rates were lower (see the Supporting Information).

To explain the short lag time observed (ca. 0.5 ms; Figure 1a), we propose that the positively charged [Ru(bpy)₃]³⁺ moiety directly forms an ion pair with the used

[*] Dr. T. Eliash, Prof. M. Sheves
Dept. of Organic Chemistry, Weizmann Institute of Science
Rehovot 76100 (Israel)

Dr. A. Barbon, Prof. M. Brustolon
Dept. of Chemical Sciences, University of Padova
Via Marzolo 1, 35131 Padova (Italy)
E-mail: antonio.barbon@unipd.it

Dr. I. Bilkis
Faculty of Agricultural, Food and Environmental Sciences
Hebrew University, Rehovot 76100 (Israel)

Dr. L. Weiner
Dept. of Chemical Research Support
Weizmann Institute of Science, Rehovot 76100 (Israel)
E-mail: lev.weiner@weizmann.ac.il

[**] L.W. thanks Harry Gray for stimulating discussions, and all of the authors are grateful to both Harry Gray and Jeff Warren for critical reading of the manuscript and for constructive comments and suggestions. We thank Israel Silman for valuable discussions while writing our responses to the referees and for editing the manuscript.

Supporting information for this article is available on the WWW under <http://dx.doi.org/10.1002/anie.201210207>.

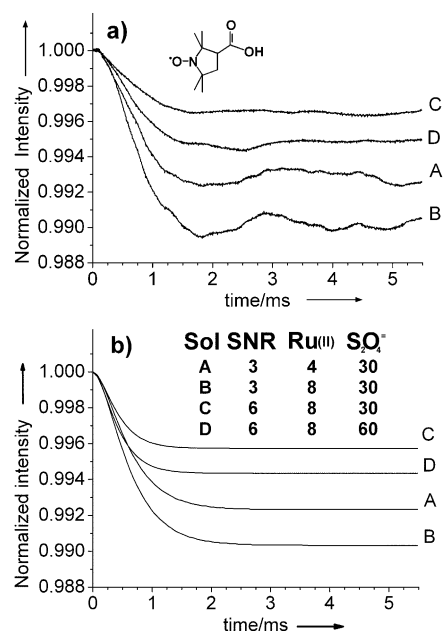
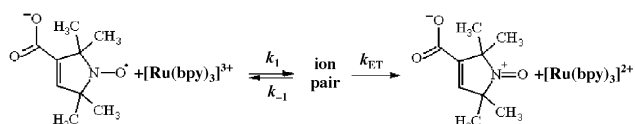


Figure 1. a) Decay of the intensity at 300 K of the normalized cw-EPR signal following a light pulse for a series of solutions containing various concentrations of the SNR, $[\text{Ru}(\text{bpy})_3]^{2+}$, and ammonium persulfate in water/ethanol 1:1. Concentrations $[10^{-4} \text{ M}]$ are shown above the simulation curves in (b). b) Simulation of the time traces employing the kinetic model discussed in the text.

nitroxyl radical. The SNR employed is a carboxylic acid, with a relatively low pK_a value of 3.4–4.^[11,12] Thus, at pH 7 it is expected to be anionic. The possibility of ion pair formation in reactions of $[\text{Ru}(\text{bpy})_3]^{2+}$ with anionic species was discussed previously.^[6,13] ET thus occurs within the ion pair, as shown in Scheme 2.



Scheme 2. Proposed electron transfer mechanism in solution.

This reaction proposal allowed us to analyze the experimental data (Figure 1b). The values of the rate constants obtained were $k_1 = (8 \pm 1) \times 10^6 \text{ L mol}^{-1} \text{ s}^{-1}$, $k_{-1} < 2 \times 10^2 \text{ L mol}^{-1} \text{ s}^{-1}$, and $k_{\text{ET}} = (4 \pm 1) \times 10^3 \text{ s}^{-1}$.

We show the analysis of the temperature dependence of k_{ET} for a water/glycerol 3:7 solution, which yields more sensitive temperature dependence in the narrow range examined. Exploring Eyring theory, which relates k_{ET}/T to the activation enthalpy (ΔH^\ddagger) and entropy (ΔS^\ddagger),

$$\ln\left(\frac{k_{\text{ET}}}{T}\right) = \left[\frac{\Delta S^\ddagger}{R} + \ln\left(\frac{k_B}{h}\right)\right] - \frac{\Delta H^\ddagger}{R} \frac{1}{T} \quad (1)$$

we plotted $\ln(k_{\text{ET}}/T)$ as function of T (see Figure 2) to obtain the activation parameters. The values of k_{ET} were obtained

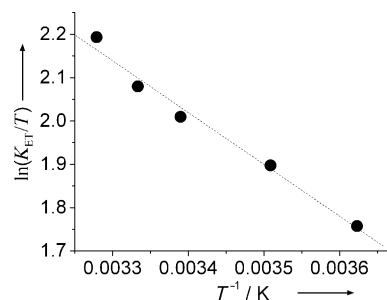


Figure 2. $\ln(k_{\text{ET}}/T)$ as a function of $1/T$ for the oxidation of the SNR by $[\text{Ru}(\text{bpy})_3]^{2+}$ in a water/glycerol 3:7 solution. The dashed line shows linear fitting to the data.

from the simulations of the decay curves (see Supporting information).

We were thus able to obtain values of $\Delta H^\ddagger = 10 \pm 1 \text{ kJ mol}^{-1}$ and $\Delta S^\ddagger = 0.147 \pm 0.003 \text{ kJ mol}^{-1} \text{ K}^{-1}$, from which a free activation energy for ET, $\Delta G^\ddagger = 54 \pm 6 \text{ kJ mol}^{-1}$, was determined.

According to the Marcus theory,^[1] as described in the Supporting Information, resorting the ΔG^0 value from the redox potential of the pair, we also obtained a reorganization energy value of $\lambda = 2.4 \pm 0.5 \text{ eV}$ at 270 K. This value is in agreement with published data for $\text{R}_2\text{N-O}^\bullet/\text{R}_2\text{N-O}^+$ and $[\text{Ru}(\text{bpy})_3]^{2+}/[\text{Ru}(\text{bpy})_3]^{3+}$ self-exchange reactions in aqueous solutions.^[14,15]

In proteins, the electron-transfer mechanism is normally different from that in solution if the two partners are sufficiently separated. The reason is that ET processes in proteins over long distances can occur via tunneling. Normally, two possible pathways are considered: a through-space route and a through-bonds route.^[2,5] The latter is dominant in the presence of an efficient hydrogen-bond network, such as those present in organized protein structures, for example, α -helices or β -sheets.^[2] In such cases, there is a linear relation between the logarithm of k_{ET} and the donor/acceptor distance, and quite high rates can be observed, even for partners separated by tens of Ångströms.^[2]

We made use of bacteriorhodopsin (bR) as a model system to apply the above method to studying ET in a biological system; the choice lies on the following reasons: 1) Divalent cations like Ca^{2+} , Mg^{2+} , and Mn^{2+} form stable complexes with the protein without altering its structure and function; 2) the distances of the coordinated ions to spin labels on the protein were determined earlier;^[16] 3) $[\text{Ru}(\text{bpy})_3]^{2+}$ replaces these ions without affecting the structure of the protein;^[9] and 4) the X-ray structure of bR is known and can be used to explain the electron transfer data. We believe however that the approach applied to bR in this work could be applied to other biological systems.

Two strongly bound Ca^{2+} ions, bound on the surface of the bR protein (one bound at the extracellular side, and the second at the protein cytoplasmic side,^[16] were fully replaced by two Ru complexes without any major effect on the structure of the protein.^[9] Accordingly, the following controls were performed: 1) Addition of $[\text{Ru}(\text{bpy})_3]^{2+}$ to deionized bR changed the protein absorption spectrum from blue to purple,

just as happens on addition of Ca^{2+} ; 2) Mn^{2+} can displace bound Ca^{2+} ^[16] and $[\text{Ru}(\text{bpy})_3]^{2+}$ displaces the bound Mn^{2+} located at the cytoplasmic side of bR; and 3) high concentrations of Ca^{2+} significantly decreased or prevented binding of $[\text{Ru}(\text{bpy})_3]^{2+}$ to bR and produced a considerable decrease in the rate of oxidation of the SNR. The SNR donor was attached at different positions in the protein by use of two approaches. The first used site-directed mutagenesis to attach a spin label to residue 103 at the protein cytoplasmic side, that had been converted from alanine into cysteine (A103C); the second approach involved substitution of the covalently bound retinal chromophore by a spin-labeled synthetic analogue^[16] (see insert in Figure 3b).

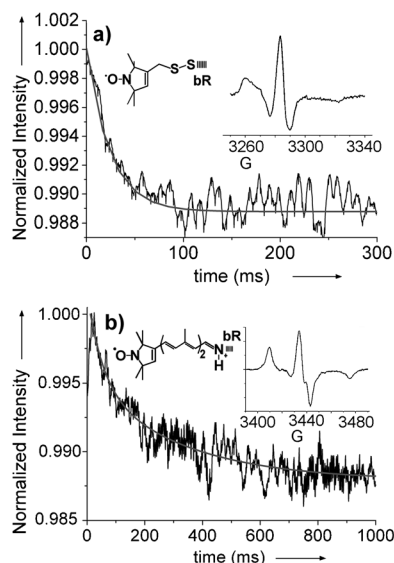


Figure 3. Time dependence of the decrease in cw-EPR intensity following a light pulse at room temperature for the bR mutant spin-labeled at residue 103 (a), and for the bR bearing the spin-labeled retinal analogue (b). The corresponding insets show the EPR signals of the immobilized spin probes.

In the case of the spin-labeled mutant 103C the donor/acceptor pair are close to each other, but probably without a connection by a α -helix or β -sheet-mediated hydrogen-bond network; in the case of the spin labeled chromophore analogue, they are distant from each other, but are likely at two ends of an α -helix (Figure 4).

Figure 3a and b show that in both spin-labeled bR derivatives the decay of the cw-EPR signal follows a simple monoexponential time course, as would be predicted for a direct exchange process.^[2,5] The ET rate constants thus determined were $k_{\text{ET}} = (2 \pm 1) \times 10^3 \text{ s}^{-1}$ for the spin-labeled moiety attached to residue 103 and $k_{\text{ET}} = (1.2 \pm 0.5) \times 10^1 \text{ s}^{-1}$ for the spin-labeled retinal analogue inserted at the active site.

For the bR labeled at residue 103C, ET is rather slow compared to α -helix or β -sheet-mediated ET.^[2,5] For a theoretical estimation of k_{ET} , we used the experimentally proposed distances between bound Mn^{2+} proposed to be located at the Asp36, Asp38 locus^[17] at the cytoplasmic side (15.1 Å) and the

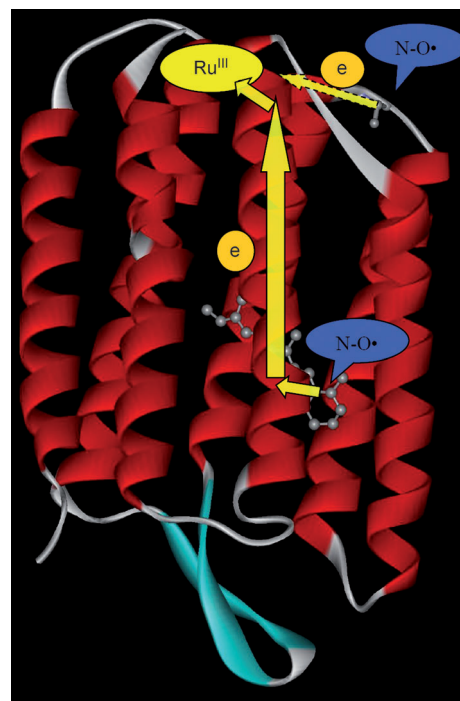


Figure 4. Proposed mechanism for electron transfer from a spin-labeled donor attached to bacteriorhodopsin to a $[\text{Ru}(\text{bpy})_3]^{3+}$ complex acceptor on its surface. A 1.55 Å crystal structure of bR (PDB code: 1C3W) is displayed in cartoon format. The $[\text{Ru}(\text{bpy})_3]^{3+}$ complex is attached on the cytoplasmic face of the membrane. Two bound nitroxyl residues (blue label) are also depicted. One is attached covalently to a Cys inserted at position 103 by site-directed mutagenesis; the other is a spin-labeled analogue of retinal that replaces the native chromophore at the active site. The yellow arrows depict the two possible directions of electron transfer.

spin label inserted at the 103 residue and between bound Mn^{2+} and the spin label inserted at the active site (22 Å),^[16] assuming that these distances are maintained when the Mn^{2+} is displaced by $[\text{Ru}(\text{bpy})_3]^{2+}$. For these distances, α -helix k_{ET} values larger than $2 \times 10^6 \text{ s}^{-1}$ and $2 \times 10^1 \text{ s}^{-1}$, respectively, can be predicted^[2] (see the Supporting Information). The satisfactory agreement between the theoretical and experimental values of k_{ET} for the bR spin labeled at the active site indicates that this could be a classical case of α -helix-mediated ET^[2] (Figure 4). The much lower k_{ET} value observed experimentally for the labeled bR 103C mutant can be ascribed to the absence of an efficient hydrogen-bond network between the nitroxyl radical and the $\text{Ru}(\text{bpy})_3^{3+}$ complex^[2,5] (Figure 4).

Assuming an ET through water for 103C, we can obtain a value^[2] $k_{\text{ET}} \approx 10^4 \text{ s}^{-1}$. Indeed, along with the distance, for ET other very important factors, such as protein fold, can be the key determinant of biological ET rates: they establish the driving force, the reorganization energy, and the electronic coupling.^[2]

To summarize, a novel method is presented for measuring ET rates by use of time-resolved EPR, which involves photooxidation of SNRs by ruthenium complex. In solution, the method was used to generate the fundamental characteristics of the ET process. It was further validated in measure-

ments on two spin-labeled derivatives of bR. A relevant issue is the general applicability of the method. Whereas the range of oxidation potentials of 5- and 6-membered ring nitroxyls is 0.5–0.8 V,^[4,18] the range of oxidation potentials of various ruthenium complexes is 1.1–1.7 V.^[4,19] Thus, the range of differences in oxidation potentials is $\Delta E_{1/2} \approx 0.3$ –1.2 V. Consequently, from a thermodynamic point of view, oxidation of nitroxyl residues by ruthenium complexes is always allowed. This gives the ample opportunity for studying the dependence of the rate of the ET reaction on ΔG^0 for the Ru³⁺/SNR pair.

Thus, this approach can be applied to the study of ET in proteins, nucleic acids, and biological membranes. It is noteworthy that EPR spectra of some SNRs (for example, imidazoline and imidazolidine derivatives) are pH-sensitive.^[20] These latter probes may be used for simultaneous study of electron transfer and proton transfer, making use of time-resolved EPR. This may provide a unique approach to characterization of proton-coupled ET reactions.^[21]

Received: December 21, 2012

Revised: May 22, 2013

Published online: July 1, 2013

Keywords: electron transfer · EPR spectroscopy · kinetics · nitroxyl radicals · ruthenium

- [1] R. A. Marcus, N. Sutin, *Biochim. Biophys. Acta Rev. Bioenerg.* **1985**, 811, 265–322.
- [2] H. B. Gray, J. R. Winkler, *Q. Rev. Biophys.* **2003**, 36, 341–372.
- [3] C. Wei, A. J. Bard, M. V. Mirkin, *J. Phys. Chem.* **1995**, 99, 16033–16042.
- [4] W. Ford, M. Rodgers, *J. Phys. Chem. B* **1997**, 101, 930–936.
- [5] H. Gray, J. Winkler, *Chem. Phys. Lett.* **2009**, 483, 1–9.
- [6] H. S. White, W. G. Becker, A. J. Bard, *J. Phys. Chem.* **1984**, 88, 1840–1846.
- [7] M. C. Krishna, D. A. Grahame, A. Samuni, J. B. Mitchell, A. Russo, *Proc. Natl. Acad. Sci. USA* **1992**, 89, 5537–5541.
- [8] A. P. Todd, J. Cong, F. Levinthal, C. Levinthal, W. L. Hubbell, *Proteins Struct. Funct. Genet.* **1989**, 6, 294–305.
- [9] X. Fu, S. Bressler, M. Ottolenghi, T. Eliash, N. Friedman, M. Sheves, *FEBS Lett.* **1997**, 416, 167–170.
- [10] I. Ron, L. Sepunaru, S. Itzhakov, T. Belenkova, N. Friedman, I. Pecht, M. Sheves, D. Cahen, *J. Am. Chem. Soc.* **2010**, 132, 4131–4140.
- [11] R. N. Schwartz, M. Peric, S. A. Smith, B. L. Bales, *J. Phys. Chem. B* **1997**, 101, 8735–8739.
- [12] G. Saracino, A. Tedeschi, *J. Phys. Chem. A* **2002**, 106, 10700–10706.
- [13] A. L. Kaledin, Z. Huang, Y. V. Geletii, T. Lian, C. L. Hill, D. G. Musaev, *J. Phys. Chem. A* **2010**, 114, 73–80.
- [14] H. O. Finklea, N. Madhiri, *J. Electroanal. Chem.* **2008**, 621, 129–133.
- [15] R. C. Young, F. R. Keene, T. J. Meyer, *J. Am. Chem. Soc.* **1977**, 99, 2468; H. Oberhofer, J. Blumberger, *Angew. Chem.* **2010**, 122, 3713–3716; *Angew. Chem. Int. Ed.* **2010**, 49, 3631–3634.
- [16] T. Eliash, L. Weiner, M. Ottolenghi, M. Sheves, *Biophys. J.* **2001**, 81, 1155–1162.
- [17] F. Sepulcre, A. Cordoní, M. G. Proietti, J. J. Perez, J. García, E. Querol, E. Padrós, *Proteins Struct. Funct. Bioinf.* **2007**, 67, 360–374.
- [18] S. Manda, I. Nakanishi, K. Ohkubo, H. Yakumaru, K. Matsumoto, T. Ozawa, N. Ikota, S. Fukuzumi, K. Anzai, *Org. Biomol. Chem.* **2007**, 5, 3951–3955.
- [19] E. Eskelinen, M. Haukka, T.-J. J. Kinnunen, T. A. Pakkanen, *J. Electroanal. Chem.* **2003**, 556, 103–108.
- [20] L. Weiner, *Appl. Magn. Reson.* **2007**, 31, 357–373.
- [21] J. M. Mayer, *Annu. Rev. Phys. Chem.* **2004**, 55, 363–390.